ISSN 1063-7761, Journal of Experimental and Theoretical Physics, 2006, Vol. 103, No. 2, pp. 278–291. © Pleiades Publishing, Inc., 2006.
Original Russian Text © A.Ya. Parshin, V.L. Tsymbalenko, 2006, published in Zhurnal Éksperimental'noĭ i Teoreticheskoĭ Fiziki, 2006, Vol. 130, No. 2, pp. 319–334.

ELECTRONIC PROPERTIES OF SOLIDS

Kinematic Multiplication of Elementary Steps on the Surface of Helium Crystals

A. Ya. Parshin[a] and V. L. Tsymbalenko[b]

[a] *Kapitza Institute for Physical Problems, Russian Academy of Sciences, Moscow, 119334 Russia*
[b] *Institute of Superconductivity and Solid State Physics, Russian Research Centre Kurchatov Institute, Moscow, 123182 Russia*
e-mail: parshin@kapitza.ras.ru

Received March 14, 2006

Abstract—The nonlinear dynamics of elementary steps on an atomically smooth crystal–liquid interface is considered within the framework of a weak coupling approximation. In fact, the proposed theory describes faceting of the interface between solid and superfluid helium at low temperatures, when dissipative processes weakly influence the dynamics of growing steps. The main results are obtained by means of numerical calculations. The law of dispersion of a step is determined and the dependence of its shape on the propagation velocity is analyzed. It is established that a kinematic multiplication of steps is possible at a sufficiently high velocity, whereby a single step becomes unstable with respect to the formation of a pair of steps of opposite signs that leads to the appearance of a new atomic layer. Under certain conditions, the collision of steps with opposite signs may lead (in addition to the usual annihilation of steps) either to the step "transfer" to the adjacent row with the formation of a new atomic layer or to the reflection of steps from each other. Thus, a qualitatively new mechanism is proposed for the growth of crystals with atomically smooth faces in the absence of renewable sources such as screw dislocations. The effect of dissipation and external supersaturation on the dynamics of steps is considered. The possibility of experimental observation of the proposed mechanisms of step multiplication, as well as their probable relation to the unusual regimes of helium crystal growth at low temperatures, are discussed.

PACS numbers: 67.80.–s, 68.08.–p

DOI: 10.1134/S1063776106080115

1. INTRODUCTION

As is well known, a faceted crystal grows due to the propagation of elementary steps over faces, continuous growth being possible either in the presence of continuously operating sources of steps (such as screw dislocations and Frank–Read sources) or by means of new step generation via two-dimensional nucleation. The steps can propagate either due to the surface diffusion or by the attachment of particles of another phase (liquid or vapor) occurring in contact with the growing crystal. Under usual conditions, the velocity of step propagation is rather low, so that the kinetic energy of this motion (being small compared to the rest energy) is frequently ignored in the analysis of step dynamics [1, 2]. Evidently, in the other limiting case, the laws of conservation of the energy and momentum admit, for an appropriate law of dispersion, the decay of a propagating step into two, three or more new steps. With allowance for the boundary conditions at infinity, we may speak of the generation of pairs of steps with opposite signs, that is, of the generation of a new atomic layer by a rapidly propagating step.

According to the classical theory of crystal growth, the growing steps do not intersect. This condition means that configurations possessing large excess energy—such as overgrowth of one atomic layer over another that corresponds to the intersection of steps of the same sign—are excluded from consideration. As for the steps of opposite signs, this condition implies that the intersection (collision) of two such steps leads to their annihilation in the region of contact, which reduces the total length and, accordingly, decreases the energy of steps. This property of steps must certainly be retained in the quasi-static case, whereby steps are propagating at a sufficiently low velocity so that every part of a step at any moment of time can be considered as occurring in equilibrium, and the kinetic energy of a step can be neglected. The quasi-static approximation implies that the relaxation time is small compared to the "collision time" w/V, where V is the relative velocity of steps and w is the characteristic step width (typically, on the order of interatomic distance). This condition is usually well satisfied, but it can be readily violated in the case of a helium crystal surface at very low temperatures, where the rate of energy dissipation tends to zero. Accordingly, the relaxation time exhibits infinite growth and, hence, the steps can propagate at very high velocities, up to the velocity of sound [3]. It is natural to suggest that, in this case, the colliding steps of oppo-

site signs are not necessarily annihilated and can either pass "by inertia" one over another, thus forming a new atomic layer (see Fig. 1), or reflect from each other.

This paper theoretically demonstrates that, under certain conditions, all the aforementioned nonclassical processes can actually take place. As a result, the growth kinetics of crystals with atomically smooth faces significantly deviates from predictions of the classical theory. In the concluding section, we will discuss the experimental opportunities offered by this circumstance. A brief outline of certain results was previously presented in [4].

2. MAIN EQUATIONS

In order to study dynamical growth processes involving elementary steps, it is necessary to develop a quite realistic model capable of describing displacements of a helium crystal surface on a microscopic scale. In formulating such a model, we must take into account that the interface between superfluid and solid helium features large quantum fluctuations [5], so that the correlation length and, hence, the effective step width become large compared to the interatomic distance [6]. Under such conditions, the most appropriate model for our purposes is that of the sine-Gordon type with a continuous variable $\zeta(\mathbf{r})$ representing the fluctuation-average local displacement of the surface relative to the equilibrium positions in an effective periodic potential that describes the surface coupling to the crystal lattice [6–8]. The effective pinning potential proves to be small as compared to the surface energy, which corresponds to the weak coupling approximation that is widely used (see, e.g., [9]) in the theory of phase transitions related to the onset of crystal faceting (roughness transition). In addition, the presence of such a variable makes it possible to apply equations of macroscopic hydrodynamics to the description of liquid motions accompanying the crystallization and melting processes.

The standard theory using the weak coupling approximation for the description of step dynamics [9, 10] does not take into account the kinetic energy of the system; that is, it restricts the consideration to quasi-stationary processes. Making allowance for the kinetic energy expands the field of applicability of the modified theory up to the limits of validity of the concept of nondissipative crystallization [5]. According to modern experimental data (see the recent review [11]), this domain extends at least up to velocities on the order of sound velocity in liquid helium ($c = 3.6 \times 10^4$ cm/s) and frequencies on the order of 10^{11} Hz. As for the permissible temperature range, this is limited only by the temperature T_R of the roughening phase transition on the surface of a given orientation (e.g., for (0001) face of a ^{4}He crystal, $T_R = 1.3$ K). In fact, below we assume everywhere except Section 4.2 that the temperature is sufficiently low to ignore the dissipation. In addition,

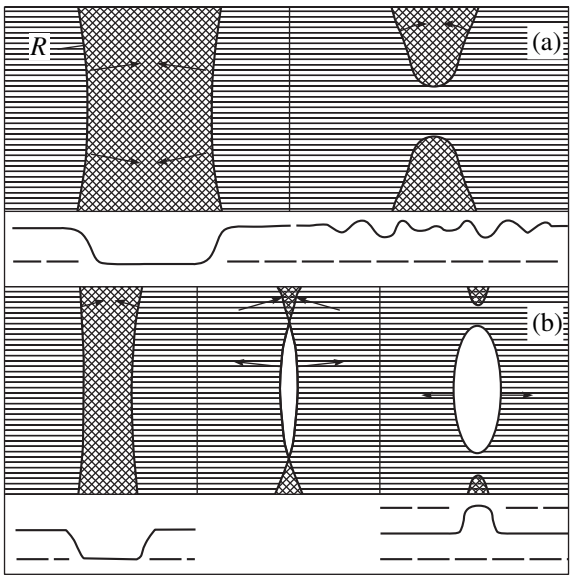

Fig. 1. Schematic diagrams illustrating the collisions of steps (a) with annihilation (a quasi-classical case) and (b) with the formation of a new layer (dynamic case). Adjacent atomic layers are indicated by different cross-hatching.

we restrict the consideration to step velocities below the velocity of sound, so that the liquid (as well as the crystal) phase can be considered incompressible.

The Lagrange function for the system under consideration can be written as

$$L = -\int\left[\frac{\alpha}{2}(\nabla\zeta)^2 + U_0\left(1 - \cos\frac{2\pi\zeta}{a}\right)\right]d^2\mathbf{r} + \int\frac{\rho^*}{2}\left(\frac{\partial\zeta}{\partial t}\right)^2 d^2\mathbf{r} + \int\frac{\rho_l}{2}v_l^2 dV, \quad (1)$$

where a is the interplanar distance (step height); α is the surface tension (we neglect the anisotropy of α and, accordingly, do not differentiate between the surface energy and stiffness); ρ_l and v_l are the density and velocity of the liquid phase, respectively; and the factor U_0 can be expressed in terms of the energy β per unit length of the immobile step:

$$U_0 = \frac{\pi^2}{16}\frac{\beta^2}{\alpha a^2}. \quad (2)$$

The last two terms in expression (1) describe the kinetic energy of the system. The first of these terms, representing the surface contribution related to the rearrangement of atoms in the surface layer on the passage from liquid to crystalline state [12], is relatively small and does not qualitatively influence the results of analysis. As for the second (volume) term, it can be transformed into a surface integral by assuming that the incompressible liquid fills the half-space $z > 0$ and by

taking into account the mass conservation in the course of crystallization:

$$\int\frac{\rho_1}{2}v_1^2 dV = \frac{(\rho_c-\rho_1)^2}{4\pi\rho_1} \times\int\frac{\partial\zeta(t,\mathbf{r})}{\partial t}\frac{\partial\zeta(t,\mathbf{r}')}{\partial t}\frac{d^2\mathbf{r}d^2\mathbf{r}'}{|\mathbf{r}-\mathbf{r}'|}, \quad (3)$$

where ρ_c is the helium crystal density. Retaining only this term in the kinetic energy, we obtain the equation of motion for the crystal surface,

$$\frac{1}{2\pi}\int\frac{\partial^2\varphi(t,\mathbf{r}')}{\partial t^2}\frac{d^2\mathbf{r}'}{|\mathbf{r}-\mathbf{r}'|} - \Delta\varphi + \sin\varphi = 0, \quad (4)$$

and the corresponding integrals of motion—the total energy

$$E = \frac{1}{4\pi}\int\frac{\partial\varphi(t,\mathbf{r})}{\partial t}\frac{\partial\varphi(t,\mathbf{r}')}{\partial t}\frac{d^2\mathbf{r}d^2\mathbf{r}'}{|\mathbf{r}-\mathbf{r}'|} + \int\left[\frac{1}{2}(\nabla\varphi)^2 + 1 - \cos\varphi\right]d^2\mathbf{r} \quad (5)$$

and the total momentum

$$\mathbf{P} = -\frac{1}{2\pi}\int\nabla\varphi(t,\mathbf{r})\frac{\partial\varphi(t,\mathbf{r}')}{\partial t}\frac{d^2\mathbf{r}d^2\mathbf{r}'}{|\mathbf{r}-\mathbf{r}'|}. \quad (6)$$

The dimensionless coordinates x and y in Eqs. (4)–(6) are measured in units of ξ, and the dimensionless time, in units of τ:

$$\xi = \sqrt{\frac{\alpha a^2}{4\pi^2 U_0}}, \quad \tau = \sqrt{\frac{(\rho_c-\rho_1)^2}{\rho_1}\frac{a^2}{4\pi^2 U_0}}\xi, \quad \varphi = \frac{2\pi\zeta}{a}. \quad (7)$$

For the (0001) face of the ^{4}He crystal, the values of parameters are as follows: $\alpha = 0.25$ erg/cm^2 [13–15], $\beta/a = 0.014$ erg/cm^2 [15], and

$$U_0 \approx 1.5\times10^{-3}\alpha, \quad \xi \approx 4a, \quad \tau \approx 5\times10^{-12}\ \text{s}, \quad V_0 = \xi/\tau \approx 2.8\times10^4\ \text{cm/s} < c \approx 3.6\times10^4\ \text{cm/s}. \quad (8)$$

It should be noted that Eq. (4) was obtained using the condition $|\nabla\zeta| \ll 1$, or $|\nabla\varphi| \ll 2\pi\xi/a$. Taking into account the numerical values (8), we can conclude that this condition is well satisfied for the (0001) face, since the characteristic values of $|\nabla\varphi|$ in Eq. (4) are in the general case on the order of unity. On the other hand, the condition of applicability of the weak coupling approximation, which is expressed as $a/\xi \ll 1$, is satisfied for this face with a small margin. Moreover, V_0 is only slightly below the velocity of sound in liquid helium. For these reasons, the results presented below offer only a qualitatively correct description of the properties of steps on the (0001) face. As for the other faces, the corresponding values of U_0 and, hence, V_0 are significantly lower [11], which ensures validity of all the necessary conditions.

Real steps on the crystal surface are always slightly curved, but the curvature is usually so small that the curvature radius R is large compared to ξ. In this case, it is possible to ignore in Eq. (4) the dependence on one of the coordinates (e.g., on y). The integral exhibits logarithmic divergence and should be truncated either at the face size (provided that it is smaller than R) or at R (expressed in ξ units, which eventually yields

$$\frac{1}{\pi}\int\ln\left(\frac{R}{|x'-x|}\right)\frac{\partial^2\varphi}{\partial t^2}dx' = \frac{\partial^2\varphi}{\partial x^2} - \sin\varphi. \quad (9)$$

3. METHODS OF NUMERICAL SOLUTION

The entire variety of numerical calculations can be subdivided into three types in terms of complexity. A simpler case was used to verify the correctness of solution obtained for a more complex variant. These types are as follows: (i) stationary motion of a single step (one-dimensional problem); (ii) evolution of an arbitrary profile (one-dimensional problem); and (iii) a symmetric two-dimensional (2D) problem.

3.1. Stationary Case

The general one-dimensional equation of motion (9) for the stationary propagation of a single step at a velocity V can be reduced to an ordinary integro-differential equation and written as

$$\frac{d^2 f}{dx^2} - \sin f = \frac{V^2}{\pi}\int\ln\left(\frac{R}{|x-x'|}\right)\frac{d^2 f}{dx'^2}dx' = \frac{V^2}{\pi}\int\frac{df}{dx'}\frac{1}{x'-x}dx', \quad (10)$$

where $\varphi = f(x - Vt)$, $\varphi(-\infty) = 0$, $\varphi(+\infty) = \pm2\pi$. The profile f was determined by iterations using the target method in the following sequence. The initial approximation was chosen in the form of an immobile step profile

$$f_0 = 4\arctan e^x \quad (11)$$

and used to calculate the convolution in the right-hand part of Eq. (10). Then, the equation was integrated

using the fourth-order Runge–Kutta method with an $f'(0)$ slope at the initial point. The derivative was chosen so as to fit the solution at the end of the interval $x = 20$ to the asymptotic behavior, which is described (according to Eq. (10)) by the following expression:

$$f(x) \sim \pi(1 + \mathrm{sgn}(x)) + \frac{2V^2}{x}. \tag{12}$$

The obtained solution was substituted into the right-hand part of Eq. (10) and the procedure was repeated. For the velocities $V < 1$, the convergence is exponential, which implies that the slope at $x = 0$ depends on the number of iterations as is well approximated by the formula

$$f'_n = f'_\infty - \mathrm{const}\exp\left(-\frac{n}{p}\right), \tag{13}$$

where $p \sim 1$ for the velocities $V \le 0.9$. For somewhat greater V, the rate of convergence decreases and the parameter p reaches ~5 for $V \approx 1$. For still greater velocities, we failed to find a stationary profile using this simple method.

3.2. Evolution of a One-Dimensional Profile

Physically reasonable processes of collision, annihilation, and reflection of steps under arbitrary initial conditions and velocities lead to the surface profile of a general form, so that it is necessary to solve Eq. (9) directly. For solving problems of this type, we have developed a finite difference scheme of integration. In the symmetric case, it is possible to implement a more effective Fourier transform and, in addition, to estimate the accuracy of employed calculation algorithms.

In the general case, Eq. (9) can be converted using the Hilbert transform to the following form with an explicit derivative with respect to time:

$$\frac{\partial^2\varphi}{\partial t^2} = -\frac{1}{\pi}\int\frac{\partial}{\partial x'}\left(\frac{\partial^2\varphi}{\partial x'^2} - \sin\varphi\right)\frac{dx'}{x' - x}. \tag{14}$$

Integrating by parts, we obtain a cumbersome expression that is nevertheless more convenient for constructing an effective calculation scheme:

$$\frac{\partial^2\varphi}{\partial t^2} = -\frac{1}{\pi}\int\left[\left(\frac{\partial^2\varphi}{\partial x^2} - \sin\varphi\right)\Big|_{x'} - \left(\frac{\partial^2\varphi}{\partial x^2} - \sin\varphi\right)\Big|_{x}\right]\frac{dx'}{(x' - x)^2}, \tag{15}$$

where a singular kernel in the integrand converges as $1/x^2$. Since we assume that the profile is described by a continuous function possessing continuous derivatives at least up to the fourth order, the expression in the right-hand part of Eq. (15) (as well as in Eqs. (14) and (10)) is principal-value integrable. Replacing derivatives by second-order finite differences, we constructed an explicit scheme of solution with a temporal step Δt and a spatial step Δx. The general integration formulas (trapezoidal, etc.) without allowance for the kernel singularity do not provide for the necessary accuracy of convolution calculations and lead to unstable solutions. For this reason, the integration was performed using an algorithm described in Appendix. The solution is stable (robust) provided that

$$\frac{\Delta t^2}{\Delta x^3} < 1, \tag{16}$$

which is analogous to the Courant condition for the hyperbolic equations. In most cases, the coordinate step was $\Delta x = 0.1$ and the temporal step was $\Delta t = 0.02$, while the number of nodes in the finite difference scheme grid was varied between 1000 and 10000 depending on the system evolution scale. The solution accuracy was evaluated on a grid with a spatial step of 0.05 and a temporal step of 0.005. The differences did not exceed 1%.

In the case of collision of symmetric steps with equal and opposite velocities, we used effective Fourier transform techniques. Equation (14) for the Fourier components takes the following form:

$$\frac{d^2\varphi_k}{dt^2} + |k|^3\varphi_k = -|k|F_k(\sin\varphi), \tag{17}$$

where φ_k is the profile harmonic with a wavevector k and $F_k(\sin\varphi)$ is a Fourier transform for the sine of the profile. In these terms, the problem reduces to solving a system of ordinary differential equations coupled by a function in the right-hand part. At each time step, integration of the system of equation was followed by an inverse Fourier transform that restored the step profile. Then, the Fourier transform of the sine of this function was used to construct the next iteration. The even character of φ allowed using fast Fourier transform with respect to cosine only.

As was noted above, the correctness and convergence of calculation methods was checked on test problems. For the method described in this section, the test consisted in calculating step profiles for a series of velocities and comparing the established profile with the results obtained in a stationary case as described in Section 3.1 for the initial profile corresponding to an immobile step (11). Another criterion of accuracy was provided by a comparison of the scenarios of symmetric collisions of steps obtained by both methods. The results of such verification showed that a disadvantage of the proposed algorithm in application to an arbitrary profile was an insufficiently high accuracy of convolu-

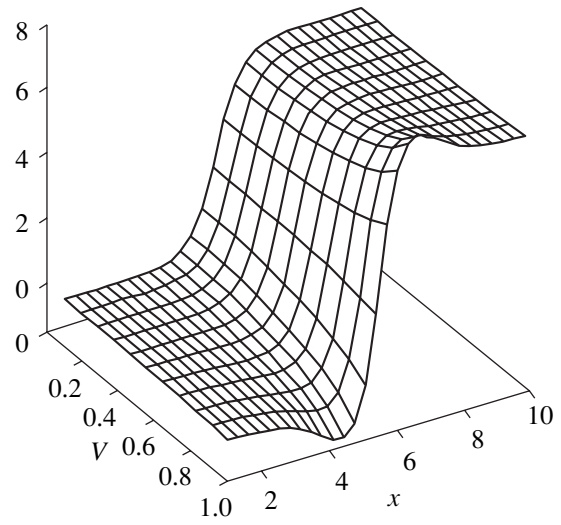

Fig. 2. Profiles of single steps uniformly propagating at various velocities. Vertical scale corresponds to an interplanar spacing of 2π.

tion calculations, which led to smoothening of the step profile and a related increase in the critical values of velocities (see below). A comparison of the results of calculations using this scheme to those provided by the more accurate calculations of step profile, energy, and momentum for a stationary step (Section 3.1) and the calculations of symmetric step collisions gave an estimate of the solution accuracy. The maximum difference between the obtained values of parameters did not exceed 10%, which can be considered as the accuracy provided by the given computational scheme.

An additional criterion of correctness for the obtained solution consisted in the verification of the law of energy conservation as

$$E = \frac{1}{2\pi}\int \ln\left(\frac{R}{|x'-x|}\right)\frac{\partial\varphi(x)}{\partial t}\frac{\partial\varphi(x')}{\partial t}dxdx' + \int\left[\frac{1}{2}\left(\frac{\partial\varphi}{\partial x}\right)^2 + 1 - \cos\varphi\right]dx. \quad (18)$$

This check was made for several velocities and showed that the energy remained constant with time to within 5–10%, which provided an additional estimate for the solution accuracy.

3.3. Two-Dimensional Case

Calculations of the propagation of steps in the 2D case require significantly greater computational facilities as compared to the one-dimensional case. This circumstance restricted our possibilities to solving a symmetric problem for colliding steps. The high symmetry of the problem made possible the use of an effective method based on the Fourier transform analogous to that described in the preceding section. In the general case, the equation of motion was as follows:

$$\frac{1}{2\pi}\int\frac{\partial^2\varphi}{\partial t^2}\frac{d^2\mathbf{r}'}{|\mathbf{r}-\mathbf{r}'|} = \Delta\varphi - \sin\varphi. \quad (19)$$

Applying the Fourier transform, we obtain

$$\frac{d^2 f_{km}}{dt^2} + |\mathbf{k}|^3 f_{km} = -|\mathbf{k}|F_{km}(\sin\varphi), \quad (20)$$

where f_{km} is the amplitude of a harmonic with the wavevector $\mathbf{k}$. We obtained a system of $M \times N$ ordinary differential equations. Owing to the symmetry of the problem, the expansion into series was performed for cosines only, which reduced the number of equations by half. Specific features of the Fourier transform additionally reduced this number by a factor of 4.

The solution algorithm was verified by solving a one-dimensional problem (one-dimensional step moving in the 2D case, profile determination, symmetric collisions). The obtained solutions showed good coincidence (to within the accuracy indicated above) both with respect to the evolution of step profiles and the values of critical velocity.

4. MODELING THE MOTION OF A SINGLE STEP

4.1. Profile, Energy, and Momentum of a Single Step

A solution to Eq. (1) for $V = 0$ is a monotonic function of x. As the velocity increases, the profile acquires two symmetric humps (Fig. 2) and decays at the infinity according to a power law (instead of the exponent) according to Eq. (12). Substituting this profile into expressions for the energy and momentum,

$$E = \frac{MV^2}{2} + \int\left[\frac{1}{2}\left(\frac{\partial\varphi}{\partial x}\right)^2 + 1 - \cos\varphi\right]dx, \quad P = MV, \quad (21)$$

with the parameter M expressed as

$$M = \frac{1}{\pi}\int \ln\left(\frac{R}{|x'-x|}\right)\frac{\partial\varphi(x')}{\partial x'}\frac{\partial\varphi(x)}{\partial x}dxdx', \quad (22)$$

we can determine the law of dispersion. The results of these calculations are presented in Fig. 3. At small velocities, the energy is a quadratic function of the momentum. As the velocity approaches unity, this dependence becomes virtually linear ("relativistic" case). It should be noted that the parameter M is not equivalent to a "mass" per unit step length, since this quantity also depends on the profile shape, that is, on the velocity. We have separately considered the question as to how the energy and momentum values depend

on the radius of integration in Eqs. (21) and (22). It was found that the values of parameters exhibit a rather insignificant (logarithmic) dependence on the size of the integration domain. This can be illustrated by the ratios of parameters obtained using the integration domains of radii 100 (*a*) and 1000 (*b*) for two velocities: $V = 0.2$. $E_b/E_a = 1.06$, $P_b/P_a = 1.44$; $V = 0.95$. $E_b/E_a = 1.24$, $P_b/P_a = 1.32$.

4.2. Step Propagation under Conditions of Supersaturation and Dissipation

In the general case, the surface motion is accompanied by the energy dissipation. At low temperatures, the dissipation is related predominantly to the interaction with phonons. This interaction has an essentially nonlocal character and its description goes far beyond the framework of the model used in our study. For a qualitative description of the dissipation phenomena, let us introduce a term proportional to $\partial\varphi/\partial t$ into the general equation of motion (4). In the presence of dissipation, the stationary propagation of a step must be supported by a supersaturation in the system, which is equivalent to adding a constant term into the equation of motion. As a result, we obtain the following equation instead of (9):

$$\frac{1}{\pi}\int \ln\left(\frac{R}{|x-x'|}\right)\frac{\partial^2\varphi}{\partial t^2}dx' = \frac{\partial^2\varphi}{\partial x^2} - \sin\varphi + \delta - \gamma\frac{\partial\varphi}{\partial t}. \tag{23}$$

Generally speaking, friction modifies the step shape. Since the parameters δ and γ introduced in this way are small at low temperatures, the shape distortions will be small. The results of numerical calculations using the scheme outlined in Section 3.1 showed that, for $\gamma = 0.1$, the maximum velocity, and the corresponding supersaturation, the change in the profile caused by the dissipation did not exceed several percent.

The rate of variation of the total energy of the step in the presence of supersaturation and dissipation is

$$\frac{dE}{dt} = \delta\frac{d}{dt}\left(\int\varphi dx\right) - \gamma\int\left(\frac{\partial\varphi}{\partial t}\right)^2 dx. \tag{24}$$

In the stationary case, the friction losses are compensated by the supersaturation and we obtain the following relation for the velocity of step propagation:

$$V = \frac{2\pi\delta}{\gamma\int\left(\frac{\partial\varphi}{\partial x}\right)^2 dx}. \tag{25}$$

As can be seen from this formula, the velocity is proportional to the supersaturation only in the region of small values. As the velocity grows, a change in the step shape leads to deviations from the linear dependence. The results of numerical calculations of the dependence of the velocity on the supersaturation are presented in Fig. 4.

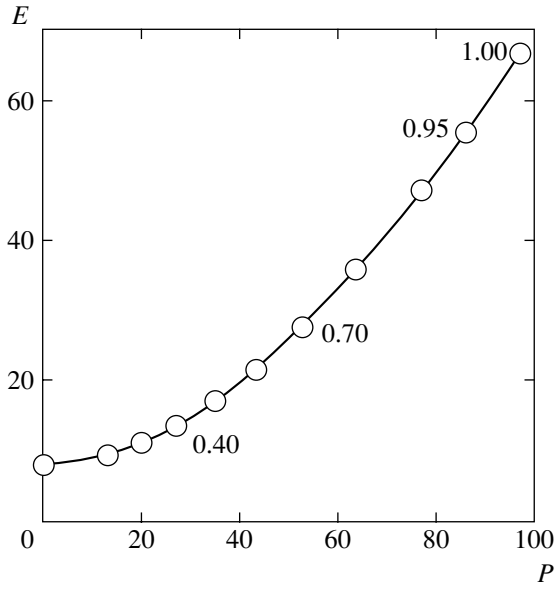

Fig. 3. A plot of the energy E versus momentum P of a single step P. Figures at the points indicate the step velocities.

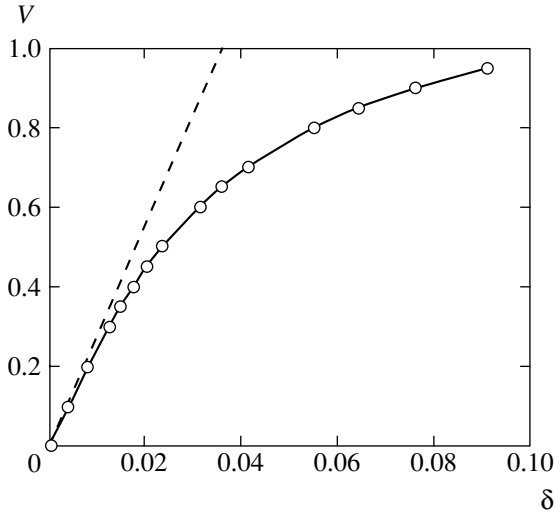

Fig. 4. Plots of the velocity of stationary motion of a single step in the presence of dissipation and supersaturation.

The presence of supersaturation leads to acceleration of the step. Let us estimate the time required for attaining a critical velocity sufficient for the appearance of a new layer. As can be seen from Fig. 3, for $V \le V_c$ the energy is approximately a quadratic function of the velocity and we can use the relation

$$\frac{dE}{dt} \approx \frac{d}{dt}\left(\frac{MV^2}{2} + \text{const}\right) \approx MV\frac{dV}{dt} = 2\pi\delta V, \quad V = \frac{2\pi\delta}{M}t. \tag{26}$$

According to this expression, the characteristic time of acceleration for the experimentally reasonable supersaturations of $\delta \le 0.1$ is on the order of $M/\delta \sim 10^3$–10^4.

4.3. Small Oscillations

The spectrum of small surface oscillations (ripplons) in the absence of steps can be readily determined by linearizing Eq. (4), which yields

$$\omega^2 = (\mathbf{k}^2 + 1)|\mathbf{k}|. \quad (27)$$

The minimum phase velocity for this law of dispersion is $\sqrt{2}$. This result implies that the motion of steps with velocities not exceeding $\sqrt{2}$ is not accompanied by the emission of ripplons.

The spectrum of small oscillations of the steps depends on the velocity of propagation. Within the framework of the model adopted, each oscillation is characterized by a wavevector q directed along the step (y axis) and by the number of the corresponding mode. Since the step profile is described by a function of the continuous variable x, there is, generally speaking, an infinite number of modes. Among these, there is one gapless mode corresponding to bending oscillations of the step. The law of dispersion on this mode for small q and arbitrary V can be determined as described below.

Let us seek for a solution to Eq. (4) in the following form:

$$\varphi = \varphi_0(x - Vt) + f(x - Vt)e^{-i\omega t + iqy}, \quad (28)$$

where f is a small deviation from the stationary profile φ_0. The linearized Eq. (4) can be written in terms of the Fourier components as

$$\left(k^2 + q^2 + 1 - \frac{(\omega + kV)^2}{\sqrt{k^2 + q^2}}\right) f_k = \int I_{k'-k} f_{k'} dk', \quad (29)$$
$$I_k = \frac{1}{2\pi}\int (1 - \cos\varphi_0(x))e^{ikx} dx.$$

For $f_k = ik\varphi_{0k} + \psi_k$, where $\psi_k \longrightarrow 0$ at $q \longrightarrow 0$ (and $\omega \longrightarrow 0$), we obtain (upon multiplying by $k\varphi_{0k}$ and integrating) the following relation:

$$\int_{-\infty}^{\infty}\left(\frac{(\omega + kV)^2}{\sqrt{k^2 + q^2}} - |k|V^2 - \frac{k^2V^2}{\sqrt{k^2 + q^2}}\right)\varphi_{0k}^2 k^2 dk = 0, \quad (30)$$

which can be rewritten as

$$\omega^2 = \frac{\int_0^{\infty}\left(q^2 + kV^2 - \frac{k^2V^2}{\sqrt{k^2 + q^2}}\right)k^2\varphi_{0k}^2 dk}{\int_0^{\infty}\frac{k^2}{\sqrt{k^2 + q^2}}\varphi_{0k}^2 dk}. \quad (31)$$

For a small velocity, we have

$$\varphi_{0k} = \frac{1}{ik\cosh(\pi k/2)},$$

which yields (in a logarithmic approximation with respect to q)

$$\omega^2 = \frac{2q^2}{\pi\ln(1/q)} + \frac{q^2V^2}{2}. \quad (32)$$

The question concerning a gap in the spectrum of "optical" oscillations is briefly considered in the next section.

4.4. Stability of Steps

As can be seen from Eq. (31), the frequency of the bending oscillations remains substantially positive for all velocities. This implies that a moving step, as well as a propagating one, is stable with respect to the onset of bending oscillations (at least log-wavelength ones). On the other hand, a step can be unstable with respect to the oscillations of some other type involving a change in the step shape (including the case of $q = 0$).

The possibility of such instabilities is related to the fact that the law of dispersion presented in Fig. 3 has a decay character. It can be shown that a minimum velocity at which the decay is possible corresponds to the separation of a step into three components with equal momenta and energies (the decay into two steps is impossible for the given boundary conditions at the infinity). This phenomenon provides a qualitatively new mechanism of step multiplication either in the same atomic layer or with the formation of a new layer, depending on which one of the three possible scenarios is realized (Fig. 5). A numerical estimate based on the spectrum of Fig. 3 gives a critical velocity of about 0.77. The fact of attainment of this critical velocity level does not imply that the process would necessarily begin. This condition only indicates that the state of a propagating isolated step becomes metastable. Decay of this state can be induced by any inhomogeneity, in particular, by a local curvature of the step. A threshold-less multiplication of steps begins upon reaching a limit of absolute instability.

Let us consider the propagation of an isolated step at a constant velocity V in the case of a deviation from the equilibrium shape φ_0:

$$\varphi = \varphi_0(x - Vt) + f(x)e^{-i\omega t}. \quad (33)$$

Assuming the deviation to be small and neglecting the terms of higher orders, we obtain the following equation of motion for this deviation:

$$-\frac{1}{\pi}\int \ln\left(\frac{R}{|x-x'|}\right)(-\omega^2 f + 2i\omega V f' + V^2 f'')dx' \quad (34)$$
$$-f'' + \cos(\varphi_0)f = 0.$$

Accomplishing the Fourier transform, we arrive at the following dispersion equation:

$$f_k\left(1 + k^2 - \frac{\omega^2 + 2V\omega k + V^2k^2}{|k|}\right) = \int f_{k'}I_{k'-k}dk', \quad (35)$$
$$I_q = \frac{1}{2\pi}\int(1 - \cos\varphi_0)e^{iqx}dx.$$

The onset of absolute instability corresponds to the case in which the frequency is zero.

However, instead of solving this equation, it was a simpler approach to model the decay of a step by directly solving the two-dimensional equation of motion (4). The small initial inhomogeneity was introduced in the form of a slight bending of the step. The results of calculations for $V = 0.95$ are presented in Fig. 6. It should be noted that a control calculation performed for a straight step propagating with the same velocity did show the appearance of a new layer within the same period of time, which agrees with the above statement concerning the metastability of such steps. As can be seen from Fig. 6, the surface begins to rise in the middle of the step (where the curvature radius is maximum). As a result, the nucleus of a new layer is formed by the time $t = 50$ and keeps growing ($t = 60$).

Numerical modeling showed only one of the three possible scenarios of step decay depicted in Fig. 5 (namely, the scenario presented in Fig. 5b). According to this variant, a new atomic layer is formed with the same sign of the leading front as that of the initial step. The critical velocity for this process at a small initial perturbation is close to unity. As for the two other variants of step decay, the question concerning the conditions for their realization has remained unstudied.

As was noted above, in solving the one-dimensional problem we failed to find a stationary step profile for $V > 1$. This velocity level probably corresponds to the point of absolute instability. An example of the evolution of a one-dimensional profile for a step propagating at a velocity of $V = 1.2$ is presented in Fig. 7, where the step moving leftward generates a nucleus of the next layer, which subsequently expands with time. It is interesting to note that a step with a double height keeps moving in the initial direction. As can be seen from Fig. 6, this peculiarity is retained in the 2D case, at least over a period of time used in the calculations. Elucidation of the question concerning stability of the double step requires additional investigation.

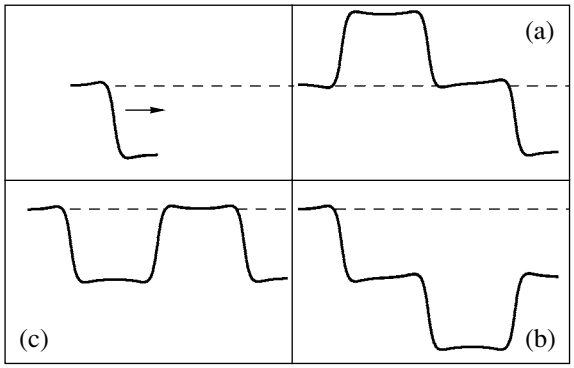

Fig. 5. Possible scenarios of step decay at a velocity above the critical value ($V = 0.77$): (a) initial step (arrow indicates the propagation direction, dashed line shows the level of growing plane); the appearance of a nucleus in the new layer behind the step front; (b) the formation of a nucleus ahead of the step front; (c) decay of a single step into three steps.

5. COLLIDING STEPS

In calculating the collisions of steps, we assumed that the supersaturation and dissipation did not significantly influence the scenarios of collisions (i.e., δ and γ values were assumed to be zero). This assumption was justified by the estimates presented in Section 4.2. As will be shown below, the collision time falls within 10–100 units. During this period, the energy of the system cannot change more than by 1%, which is within the accuracy of our calculations. Therefore, we can consider the process as the collision of steps moving by inertia.

5.1. One-Dimensional Case

In order to avoid time losses for establishing the stationary shape of steps, we used the profiles calculated for a given velocity as described in Section 3.1 as the initial approximation for the problems with colliding steps.

The collision of steps propagating with equal and opposite velocities was played using two scenarios. In the region of small velocities (until reaching a critical value), the steps always exhibited annihilation accompanied by the emission of a packet of ripplons (Fig. 8). For the velocities above the critical level (V_c), we always observed the formation of a new layer as depicted in Fig. 9. This was also accompanied by the

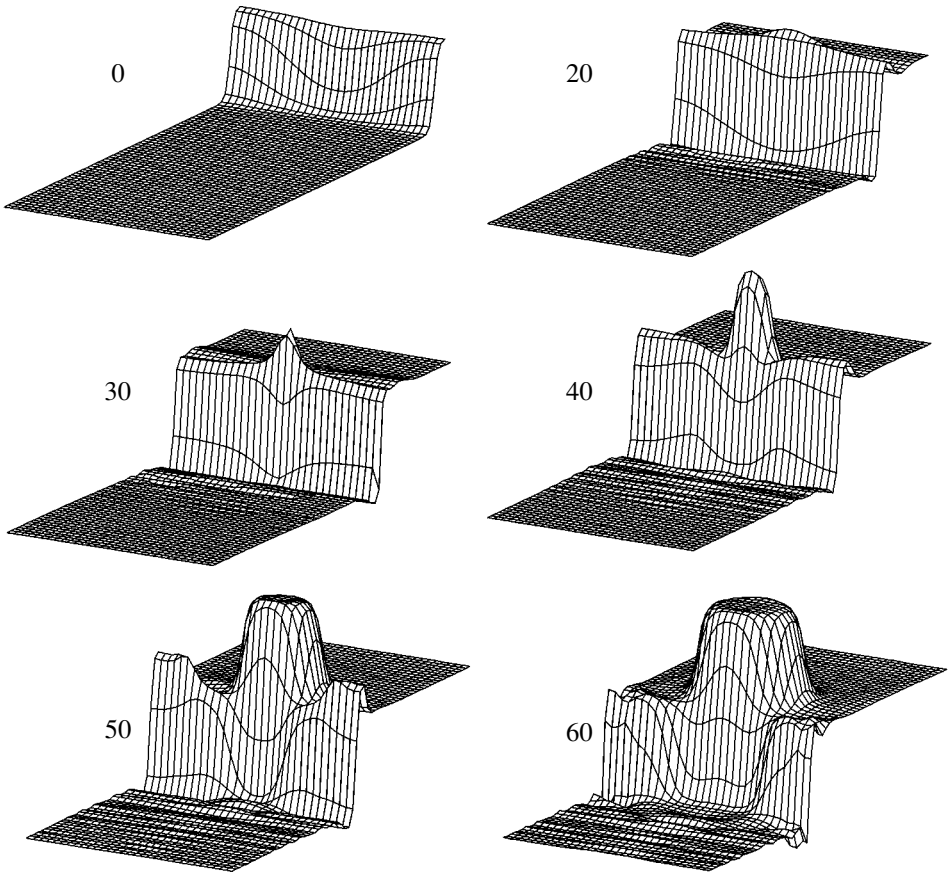

Fog. 6. Diagrams illustrating the development of instability at a velocity ($V = 0.95$) admitting the decay of a step. The initial step is slightly bent. Figures indicate the current time.

formation of ripplons, which propagated at a velocity exceeding the velocity of steps. As can be seen from Fig. 9, the velocity of steps changed rather insignificantly, so that the energy of emitted ripplons was small as compared to the energy of steps. The critical velocity determined using the Fourier method in a symmetric case was about 0.4, which was somewhat lower than the value (≈0.45) given by the general method for an arbi-

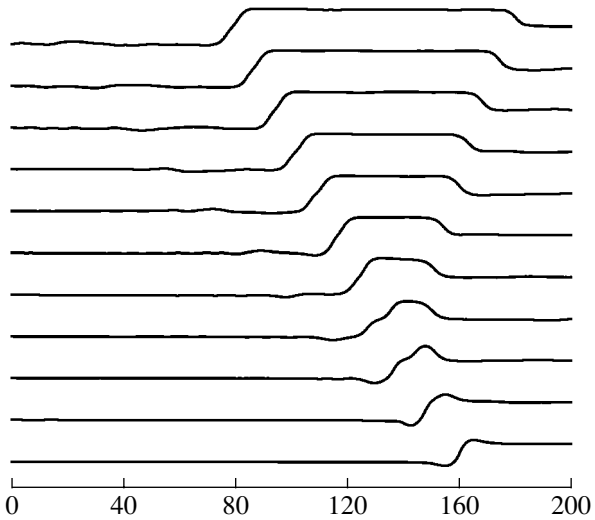

Fig. 7. The decay of a step propagating at a velocity of $V = 1.2$.

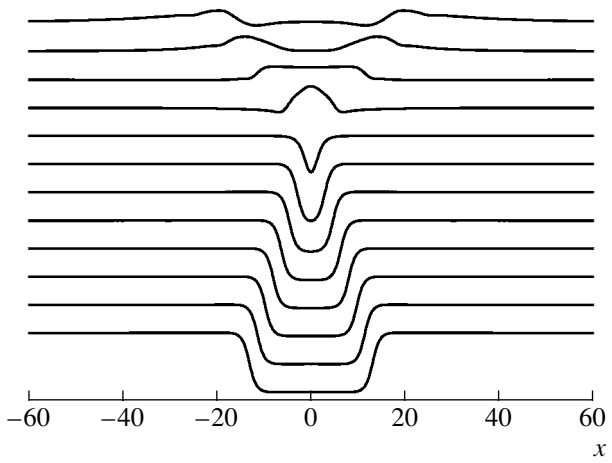

Fig. 8. Symmetric collision of steps with annihilation.

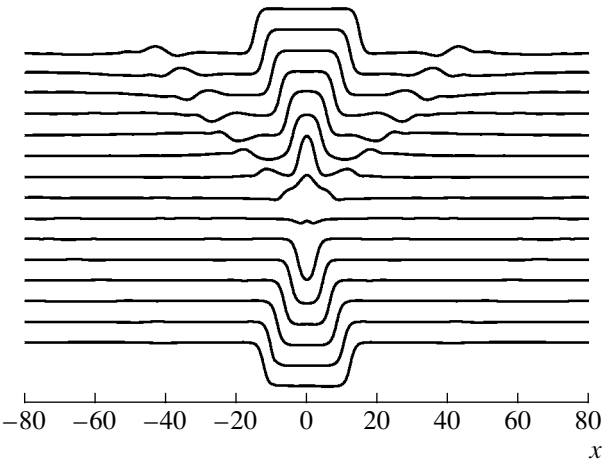

Fig. 9. Symmetric collision of steps with formation of a new layer and the emergence of ripplons. A small change in the step velocity indicates that ripplons carry away a rather insignificant part of the energy.

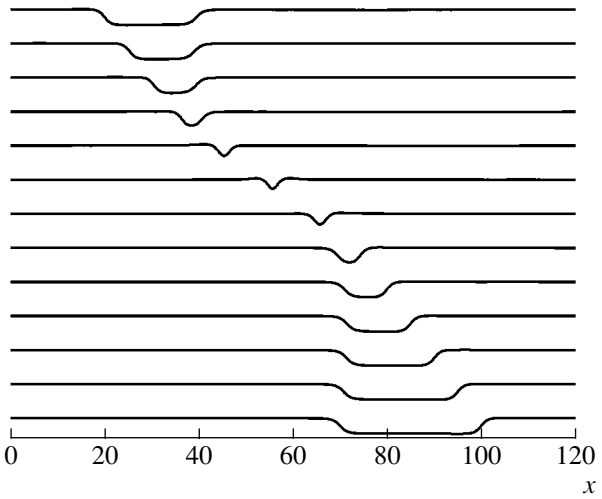

Fig. 10. Mutual reflection of steps having different velocities. As a result, the steps exchange their velocities and propagate in opposite directions.

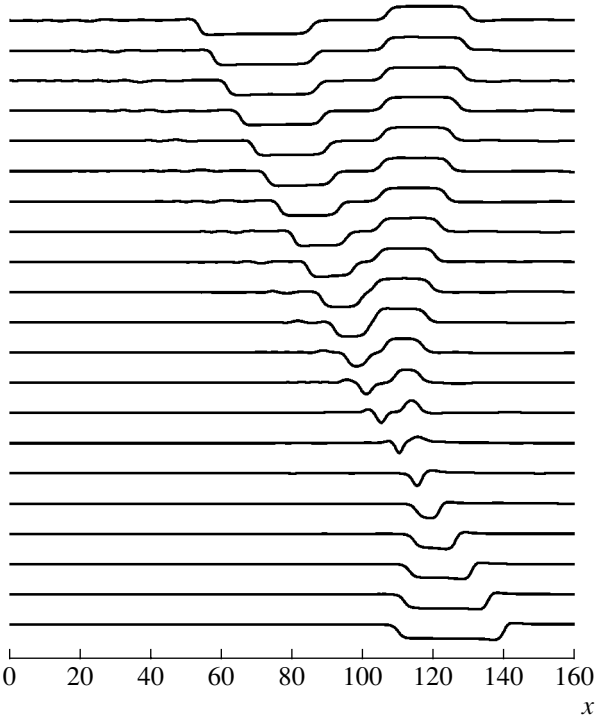

Fig. 11. Collision of steps having different velocities. As a result, a new layer is formed, the parent steps are retained in the old layer, and the newborn steps move away from the parent couple.

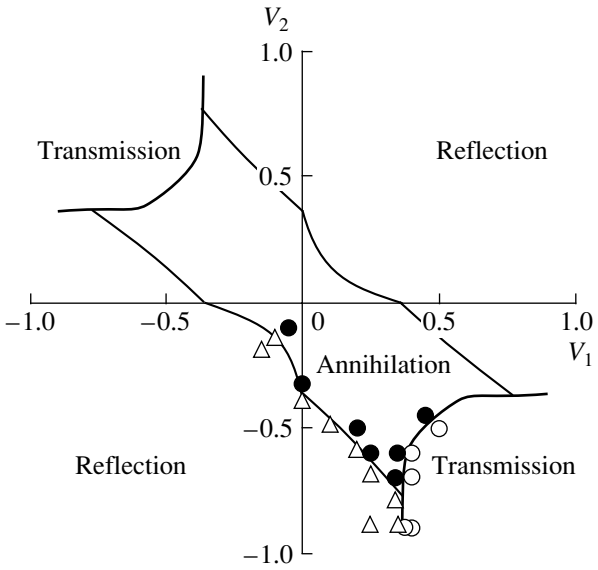

Fig. 12. Schematic diagram summarizing the results of calculations for the step collisions in the one-dimensional case. The inner region correspond to the annihilation of colliding steps. The regions of high velocities feature step transmission with the formation of a new layer; outside these regions, the steps exhibit mutual reflection.

trary step profile. To summarize these results, even the collisions of steps propagating at velocities significantly lower than the sound velocity lead to the formation of a new atomic layer and the growth of a crystal face.

As was noted above, the collisions of steps with arbitrary initial velocities were calculated using the general method. In this case, the scenarios of collision processes become more diverse. In addition to the processes of annihilation and new layer formation described in the preceding section, we observed the mutual reflection of steps and the formation of a new layer with retention of the pair of steps in the old layer (i.e., the formation of a new pair of steps). The former case is illustrated in Fig. 10. In this process, the emission of ripplons was insignificant, and the steps

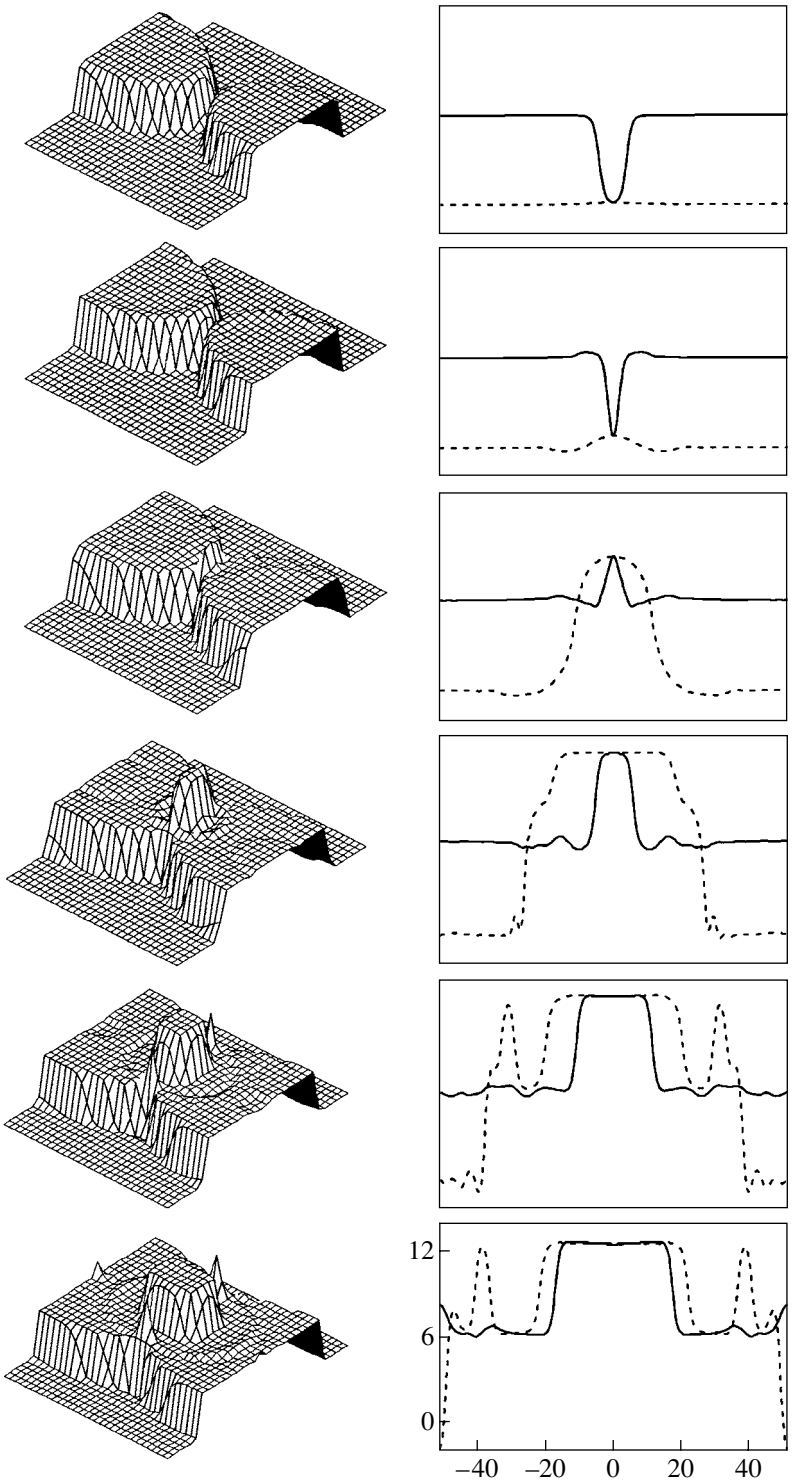

Fig. 13. Diagrams illustrating the collision of symmetric round steps propagating at $V = 0.6$. Right-hand images show the step profiles in two mutually perpendicular planes passing through the center of symmetry.

exchanged energies without practically changing their velocities. The second scenario is realized at higher velocities and the pattern is more complicated, which is illustrated in Fig. 11. Here, the initial energy is redistributed between four steps. It is interesting to note that the pair of steps in the new layer propagates in the direction determined by the left initial step.

Figure 12 gives a summary of the scenarios of collisions for arbitrary velocity relations. Regions corresponding to different regimes are apparently symmetric

relative to the bisectors of quadrants. This pattern provides the possibility of an additional evaluation of the accuracy of numerical calculations.

5.2. Two-Dimensional Case

Under real conditions, purely one-dimensional collisions of straight parallel steps considered above are low probable. Steps generated by 2D nucleation, Frank–Read sources, and spiral growth are curved. Previously, it was pointed out [4] that the collisions of steps with large radii of curvature must proceed according to a scenario close to that for the one-dimensional case. This conclusion is based on the fact that a perturbation arising at the intersection site does not accumulate with time, since the point of intersection is moving at a velocity exceeding the velocity of perturbation transfer along the steps (as long as the size of the intersection region is small compared to the curvature radius).

Verification of this statement and investigation of the collision of curved steps required the solution of a 2D problem. We used a rectangular calculation region with a side length ratio of 1 : 2 for monitoring a single collision of two ring steps with the initial velocities set along their radii. The spatial and temporal steps (0.20 and 0.02, respectively) were chosen so as to ensure stability of the algorithm (see relation (16)). In the first stage, we simulated the collisions of steps with small radii (~5). It was established that the critical velocity in this case increases to reach a level of about 0.85. The influence of the step curvature on the critical velocity value was not specially studied. In the second stage, the calculation region had dimensions 512×1024, the step radius was set to about half of the smaller size (~50), and the calculations were performed for the velocities 0.3, 0.4, and 0.6.

Figure 13 (left column) shows the evolution of the surface upon the collision of steps propagating at a velocity of 0.6; the right column presents the mutually perpendicular cross sections by planes passing through the center of symmetry of the system (solid and dashed curves refer to the profiles parallel to the short and long sides of the calculation region; the scales of all curves are identical, as indicated in the bottom right plot). The solid profile, which is perpendicular to the steps at the point of contact, is analogous to the profile obtained in a one-dimensional case. As can be seen, the temporal evolution of this profile is actually analogous to the results obtained on solving the one-dimensional problem (see Fig. 9), in agreement with what was suggested in [4]. The results of numerical calculations revealed a fine structure of the surface upon collision, which could not be determined proceeding from qualitative considerations. Indeed, the velocity of perturbation transfer along the step in the initial stage was smaller (as indicated in [4]) than the velocity of the geometric point of intersection. According to the results of calculations, this leads to a retardation of this region and the formation of the next layer, as manifested by two symmetric peaks near the nucleus of the new layer. The angle point on the intersection line is rectified rather slowly, and these peaks are retained until the end of the calculation. A detailed plot shows that waves are spreading from the angle point both along the step and over the entire surface. Once formed, the nucleus of the new layer keeps increasing in size and changes in shape from oval to spheroidal.

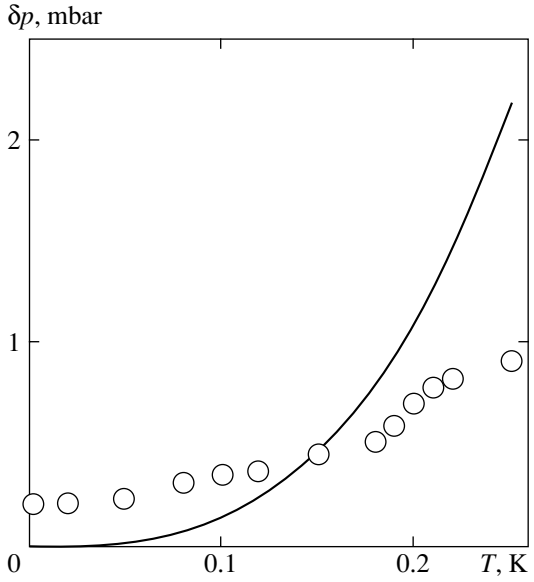

Fig. 14. A comparison of the experimental data for the "burstlike" growth [3] to the results of calculations using formula (26). Circles correspond to supersaturations at which this growth takes place. The curve shows δp values at which the stationary velocity of steps reaches a critical level of about 0.4. As can be seen, small supersaturations at temperatures below 0.15 are sufficient to accelerate steps up to velocities admitting their kinematic multiplication.

The results of calculations performed for a velocity of 0.4 showed that the central nucleus in this case is not formed, but two symmetric long-lived peaks that reach the level of the next layer appear at the point of intersection. During the time of calculations, these peaks moved away from the center of the system, neither changing in size nor decaying, showing evidence for a rather long lifetime. At a velocity of 0.3, these peaks did not reach the next layer and decayed to vanish with time.

Thus, we can ascertain that the collision of curved steps leads to the nucleation of a new layer, in agreement with what was declared previously [4]. New qualitative evidence is that the steps of smaller curvature radius must possess a higher velocity for the formation of a new crystalline layer. The appearance of peaks on the surface at the point of intersection is probably also a general property of collisions. The results of simulations revealed a large variety of scenarios of the collisions of steps propagating over a crystal surface. For example, calculations performed for the collisions of

steps having sinusoidal shapes showed that a collapse of the isolated region gives rise to a peak even at a rather small velocity. Therefore, it is not excluded that some geometric features of the steps can both increase and decrease in the critical velocity.

6. CONCLUSIONS

The results of numerical simulation of the propagation of elementary steps on the surface of helium crystals and the collisions of such steps showed that, at a sufficiently high velocity, nuclei of a new atomic layer can be generated both by a single propagating step and due to the collision of steps with opposite signs involving a "transfer" to the adjacent layer; alternatively, the colliding steps can exhibit mutual reflection from each other. Thus, a qualitatively new mechanism is proposed for the growth of crystals, which is based on the phenomenon of kinematic multiplication of elementary steps.

As was pointed out in the Introduction, the assumption that the growing steps do not intersect underlies the classical theory of growth of the atomically smooth crystal faces, in particular, the theory of spiral growth. One of the main features of this growth mechanism—a noncumulative character whereby the growth rate is independent of the number of growth dislocations—is a direct consequence of the absence of such intersections [2]. With allowance for the phenomena of kinematic multiplication of steps, the dependence of the spiral growth rate on the number of dislocations can be expected. Naturally, the dependence of the growth rate on the degree of supersaturation must change as well. Thus, the existing theoretical interpretation of the experimental data on the spiral growth of helium crystals [3] may need serious correction.

As was pointed out above, the conditions of applicability of the theory proposed in this study are well satisfied for all faces of ^{4}He crystals except for (0001), where they are valid with a small margin. Therefore, predictions of the proposed theory in this case may not be valid on a strict quantitative level. However, virtually all the available experimental data with a few exceptions refer to this very face. From this standpoint, of most interest are the experimental investigations into qualitatively new phenomena in which the predicted effects can be manifested.

The kinematic multiplication of steps probably plays an important role in the phenomenon of "burstlike" growth on a dislocation-free (0001) face of ^{4}He crystals. Figure 14 shows experimental data [3] on the average values of supersaturation for which the (0001) face exhibited a transition to the fast growth. The solid curve presents the results of calculations of a critical velocity for the step mobility (friction) taken from experimental results of the same study. As can be seen, at temperatures up to 0.15 K, the supersaturations are sufficient for accelerating the steps to a critical velocity at which their kinematic multiplication begins. At higher temperatures, the situation is reversed. However, one should not expect the exact coincidence of this approximate estimate with experiment: the process of burstlike growth has a very complicated character, which can hardly be explained by a single factor such as the appearance of a qualitatively growth mechanism on a dislocation-free crystal face. This is clear if we take into account that, for example, a transition to the fast growth takes place after a rather long action of supersaturation on the crystal face, that is, depends on the sample prehistory. However, since the observed supersaturations accelerate the steps to nearly critical velocities, the kinematic multiplication of steps is evidently a significant factor of the "burstlike" growth.

Another interesting phenomenon is the observation of anomalously high growth rates for crystal faces at temperatures within 0.2–0.8 K on a freely growing ^{4}He crystal (see short review [16]). This effect can also be related to the kinematic multiplication of steps. The whole body of experimental data available at present suggests with a high probability that the anomalous growth as well as the burstlike growth have a common physical origin. Therefore, the above considerations may equally refer to the anomalous growth. Low values of the supersaturation, which are definitely insufficient for the breakage of faceting boundaries and for the 2D nucleation, can nevertheless lead to the transformation of faces and to an increase in their growth rate by two to three orders of magnitude. At least no mechanism other that the kinematic multiplication of steps is known that can so substantially change the surface kinetics at such small deviations from the equilibrium state.

Finally, it should be also noted that recently Abe et al. [17] showed that the kinematic multiplication of steps during their collisions well explains the observed fast growth of the (0001) faces on helium crystals under the action of a high-intensity acoustic wave.

ACKNOWLEDGMENTS

The authors are grateful to A.F. Andreev, G.E. Volovik, R. Jochemsen, and V.I. Marchenko for fruitful discussions and useful advice.

This study was supported in part by the Russian Foundation for Basic Research, project no. 05-02-16806-a, and Russian President's program supporting the leading research schools (no. NSh-5763.2006.2).

APPENDIX

An integral of the type

$$I = \int \frac{f(x) - f(0)}{x^2} dx \qquad \text{(A.1)}$$

exhibits principal-value convergence, provided that the

function f is doubly continuously differentiable. We separate the singularity in the integrand as

$$I = \int_{h}^{\infty} \frac{f(x) - f(0)}{x^2} dx + \int_{-h}^{h} \frac{f(x) - f(0)}{x^2} dx + \int_{-\infty}^{h} \frac{f(x) - f(0)}{x^2} dx \quad \text{(A.2)}$$

and formulate a numerical scheme assuming that the function f is well approximated by a second-order polynomial on a segment of sufficiently small length $2h$. This approximation allows the singularity (second term in (A.2) to be integrated. The x axis is divided into segments of $2h$ length and the f function on each segment is approximated by the polynomial

$$p(x) = a_0 + a_1 x + a_2 x^2, \quad \text{(A.3)}$$

where the coefficients a_i on each segment are determined from the condition of equality of the values of f and the polynomial at the ends and in the middle of each segment. Substituting polynomials (A.3) into expression (A.2), explicitly calculating the integrals, and collecting terms, we obtain the desired numerical scheme:

$$f_n = f(nh),$$

$$I \approx \frac{1}{h} \sum_{j=-\infty}^{\infty} c_j f_j, \quad c_{-j} = c_j,$$

$$c_0 = -4, \quad c_1 = 4 - \frac{5}{4}\ln 3,$$

$$c_{2k} = 4\left[k \ln\left(\frac{2k+1}{2k-1}\right) - 1\right], \quad \text{(A.4)}$$

$$c_{2k+1} = 4 - \frac{1}{2}\left[(4k-1)\ln\left(\frac{2k+1}{2k-1}\right) + (4k+5)\ln\left(\frac{2k+3}{2k+1}\right)\right], \quad k = 1, \ldots.$$

With increasing the number n, the coefficients decrease as $1/n$.

REFERENCES

1. W. K. Burton, N. Cabrera, and F. C. Frank, Philos. Trans. R. Soc. London, Ser. A **243**, 299 (1951).
2. A. A. Chernov, in *Modern Crystallography*, Vol. 3: *Crystal Growth*, Ed. by B. K. Vaĭnshtein, A. A. Chernov, and L. A. Shuvalov (Nauka, Moscow, 1980; Springer, Berlin, 1984).
3. J. P. Ruutu, P. J. Hakonen, A. V. Babkin, et al., J. Low Temp. Phys. **112**, 117 (1998).
4. A. Ya. Parshin and V. L. Tsymbalenko, Pis'ma Zh. Éksp. Teor. Fiz. **77**, 372 (2003) [JETP Lett. **77**, 321 (2003)].
5. A. F. Andreev and A. Ya. Parshin, Zh. Éksp. Teor. Fiz. **75**, 1511 (1978) [Sov. Phys. JETP **48**, 763 (1978)].
6. S. V. Iordanskiĭ and S. E. Korshunov, Zh. Éksp. Teor. Fiz. **87**, 927 (1984) [Sov. Phys. JETP **60**, 528 (1984)].
7. E. Fradkin, Phys. Rev. B **28**, 5338 (1983).
8. D. S. Fisher and J. D. Weeks, Phys. Rev. Lett. **50**, 1077 (1983).
9. P. Nozières, *Shape and Growth of Crystals, in Solids Far from Equilibrium*, Ed. by C. Godrèche (Cambridge Univ. Press, Cambridge, 1992).
10. P. Nozières and F. Gallet, J. Phys. (Paris) **48**, 353 (1987).
11. S. Balibar, H. Alles, and A. Ya. Parshin, Rev. Mod. Phys. **77**, 317 (2005).
12. L. Puech and B. Castaing, J. Phys. Lett. **43**, L601 (1982).
13. A. V. Babkin, D. B. Kopeliovich, and P. Ya. Parshin, Zh. Éksp. Teor. Fiz. **89**, 2288 (1985) [Sov. Phys. JETP **62**, 1322 (1985)].
14. O. A. Andreeva and K. O. Keshishev, Pis'ma Zh. Éksp. Teor. Fiz. **46**, 160 (1987) [JETP Lett. **46**, 200 (1987)].
15. E. Rolley, C. Guthmann, E. Chevalier, and S. Balibar, J. Low Temp. Phys. **99**, 851 (1995).
16. V. L. Tsymbalenko, J. Low Temp. Phys. **138**, 795 (2005).
17. H. Abe, Y. Saitoh, T. Ueda, et al., J. Phys. Soc. Jpn. **75**, 023 601 (2006).

Translated by P. Pozdeev